Rab7 knockout unveils regulated autolysosome maturation induced by glutamine starvation

doi: 10.1242/jcs.215442

© 2018. Published by The Company of Biologists Ltd | Journal of Cell Science (2018) 131, jcs215442. doi:10.1242/jcs.215442

RESEARCH ARTICLE

Rab7 knockout unveils regulated autolysosome maturation induced by glutamine starvation

Yoshihiko Kuchitsu, Yuta Homma, Naonobu Fujita* and Mitsunori Fukuda*

ABSTRACT

Macroautophagy (simply called autophagy hereafter) is an intracellular degradation mechanism that is activated by nutrient starvation. Although it is well known that starvation induces autophagosome formation in an mTORC1-dependent manner, whether starvation also regulates autophagosome or autolysosome maturation was unclear. In the present study, we succeeded in demonstrating that starvation activates autolysosome maturation in mammalian cells. We found that knockout (KO) of Rab7 (herein referring to the Rab7a isoform) caused an accumulation of a massive number of LC3-positive autolysosomes under nutrient-rich conditions, indicating that Rab7 is dispensable for autophagosome–lysosome fusion. Intriguingly, the autolysosomes that had accumulated in Rab7-KO cells matured and disappeared after starvation for a brief period (∼10 min), and we identified glutamine as an essential nutrient for autolysosome maturation. In contrast, forced inactivation of mTORC1 through treatment with its inhibitor Torin2 failed to induce autolysosome maturation, suggesting that the process is controlled by an mTORC1-independent mechanism. Since starvation-induced autolysosome maturation was also observed in wild-type cells, the nutrient-starvation-induced maturation of autolysosomes is likely to be a generalized mechanism in the same manner as starvation-induced autophagosome formation. Such multistep regulatory mechanisms would enable efficient autophagic flux during starvation.

KEY WORDS: Autophagy, Autolysosome, Lysosome, Membrane traffic, Rab7

INTRODUCTION

Autophagy is an intracellular degradation system that is conserved in eukaryotes. It plays an indispensable physiological role in response to various stresses such as nutrient starvation. In the process of autophagy, isolation membranes emerge in the cytoplasm and elongate to sequester cytosolic contents. The resulting double-membrane-bound spherical structures, called autophagosomes, then fuse with endosomes and lysosomes to form hybrid organelles called amphisomes and autolysosomes, respectively. After degradation of their contents, lysosomes are reformed from the autolysosomes (reviewed in Yoshimori, 2004; Mizushima et al., 2008; Shen and Mizushima, 2014). During nutrient starvation, other steps as well as autophagosome formation must be regulated to execute autophagy, but it has remained unclear whether nutrient starvation regulates late stages of autophagy such as autophagosome or autolysosome maturation (Shen and Mizushima, 2014).

For the elimination of autophagic cargoes in autolysosomes, their degradation capacity should be upregulated to meet the rapidly increasing demand. One of the mechanisms regulating lysosomal activity during nutrient starvation is mediated by transcription factor EB (TFEB), which regulates expression of myriad genes whose products are essential to achieving lysosome homeostasis (Settembre et al., 2011; Peña-Llopis et al., 2011). However, it is questionable whether the TFEB-mediated mechanism is sufficient for proper autophagic flux, because starvation induces autophagosome formation in a transcription-independent manner, and considerable amounts of cargo is promptly transported into lysosomes.

Rab small GTPases are key regulators of intracellular membrane trafficking in eukaryotes (Fukuda, 2008; Jean and Kiger, 2012; Hutagalung and Novick, 2011). Mammals contain ∼60 Rab isoforms, and some of them have been shown to regulate autophagy (Fukuda and Itoh, 2008; Ao et al., 2014; Szatmári and Sass, 2014). One of the representative Rabs involved in autophagy is Rab7 (herein, Rab7 refers to the mammalian Rab7a isoform, a homolog of yeast Ypt7), which localizes to late endosomes/lysosomes and controls their transport and maturation (Bucci et al., 2000; Hyttinen et al., 2013; Guerra and Bucci, 2016). The role of Rab7/Ypt7 in autophagosome–lysosome fusion has been established, especially in yeast and flies (Kirisako et al., 1999; Fujita et al., 2017; Lőrincz et al., 2017). It has recently been reported that, in flies, Rab7 regulates fusion between autophagosomes and lysosomes in concert with the syntaxin17–SNAP29–VAMP8 soluble *N*-ethylmaleimide-sensitive factor attachment protein receptor (SNARE) complex, homotypic fusion and vacuole protein sorting (HOPS) tethering complex, and Rab2 (Takáts et al., 2013, 2014; Fujita et al., 2017; Lőrincz et al., 2017). Rab7 is highly conserved from invertebrates to mammals and has also been shown to be involved in autophagy in mammals (Gutierrez et al., 2004; Jäger et al., 2004; Takahashi et al., 2017). Although it is widely assumed that Rab7 also regulates fusion between autophagosomes and late endosomes/lysosomes in mammals, there is no clear or convincing evidence that mammalian Rab7 is involved in autophagosome–lysosome fusion.

In this study, we investigated the function of mammalian Rab7 in greater detail by using Rab7-knockout (KO) cells and found evidence that Rab7 is dispensable for autophagosome–lysosome fusion in cultured mammalian cells. Loss of Rab7 resulted in autolysosome accumulation, but not autophagosome accumulation, under fed conditions alone. To our surprise, nutrient-starvation induced clearance of most of the accumulated autolysosomes within ∼10 min. We also found that glutamine, but not other amino acids, is a critical nutrient for autolysosome clearance. Since regulated autolysosome clearance induced by glutamine starvation occurs irrespective of the presence or absence of Rab7, our findings suggest

Laboratory of Membrane Trafficking Mechanisms, Department of Developmental Biology and Neurosciences, Graduate School of Life Sciences, Tohoku University, Aobayama, Aoba-ku, Sendai, Miyagi 980-8578, Japan.

*Authors for correspondence (nori@m.tohoku.ac.jp; naonobu.fujita.b8@tohoku.ac.jp)

M.F., 0000-0002-8620-5853

Received 12 January 2018; Accepted 2 March 2018

Journal of Cell Science (2018) 131, jcs215442. doi:10.1242/jcs.215442

that nutrient starvation regulates autolysosome maturation in mammals in general.

RESULTS

Loss of Rab7 only blocks LC3-II flux under fed conditions and not under starved conditions

During the course of characterizing the phenotypes after loss of Rab7 in HeLa cells, we were surprised to discover that Rab7 knockdown (KD) blocked flux of LC3-II [a lipidated form of LC3 family proteins (also known as MAP1LC3 proteins, hereafter denoted simply as LC3), homologs of yeast Atg8] under fed conditions, but not under starved conditions (Fig. 1A). The LC3-II flux assay is an established protocol for assessing autophagic flux (Klionsky et al., 2016). Since bafilomycin A1, a specific inhibitor of vacuolar H^+-ATPase (V-ATPase), blocks degradation of LC3-II in lysosomes, exposing cells to bafilomycin A1 results in accumulation of LC3-II, and thus the difference in LC3-II level between cells cultured in the presence and absence of bafilomycin A1 represents the amount of LC3-II delivered to lysosomes for degradation. As previously reported, the LC3-II level in control HeLa cells increased as a result of bafilomycin A1 exposure under both fed conditions and starved conditions (Fig. 1A, lanes 1–4). In sharp contrast, the LC3-II level was much higher in fed Rab7-KD HeLa cells than in fed control cells, and its level was unaffected by the presence of bafilomycin A1 (Fig. 1A, lanes 5, 6), suggesting that the late stage of autophagy is blocked by Rab7 KD under fed conditions. To our surprise, however, normal LC3-II flux was observed in the starved Rab7-KD HeLa cells (Fig. 1A, lanes 7, 8). To confirm this finding in another cell line, we knocked out Rab7 (*Rab7a* gene) in Madin–Darby canine kidney II (MDCK-II) cells by using the CRISPR/Cas9 system (Fig. 1B). The same results were obtained as in Rab7-KD HeLa cells; LC3-II flux was blocked in the fed Rab7-KO cells, but not in starved Rab7-KO cells (Fig. 1C, lanes 1–8). As further confirmation, the Rab7-KO phenotype regarding LC3-II flux was clearly rescued by re-expression of exogenous Rab7 (Fig. 1C, lanes 9–12).

The above results imply that loss of Rab7 leads to accumulation of autophagosomes or autolysosomes under fed conditions. To observe autophagic structures in Rab7-KO cells with a confocal microscope, we immunostained Rab7-KO cells for endogenous LC3, which specifically localizes to autophagic membranes (i.e. isolation membranes, autophagosomes and autolysosomes) (Kabeya et al., 2000). As previously reported, a few LC3 puncta were observed in parental cells under fed conditions, and starvation was followed by a significant increase in their number (Fig. 2A,B). In sharp contrast to the parental cells, however, a significantly higher number of LC3 puncta was observed in fed Rab7-KO cells. Moreover, consistent with the results of the LC3-II flux assay (Fig. 1C), starvation was followed by a significant decrease in the number of LC3 puncta (Fig. 2A,B). Moreover, the creation of a mosaic system in which unmarked Rab7-KO cells and Rab7-rescued cells were plated in the same dish to compare them side by side confirmed the accumulation of LC3 puncta in the absence of Rab7 (Fig. S1A, asterisks). These findings taken together suggest that loss of Rab7 blocks the late stage of autophagy under fed conditions and that nutrient starvation induces clearance of the accumulated autophagic structures.

Starvation induces the maturation of accumulated autolysosomes in Rab7-KO cells

Rab7 is widely assumed to be essential for autophagosome maturation, especially at the autophagosome–lysosome fusion step (Gutierrez et al., 2004). To determine whether the accumulated LC3 puncta in fed Rab7-KO cells actually represent autophagosomes, we immunostained parental and Rab7-KO MDCK-II cells for both LC3 and Lamp2, a lysosomal transmembrane protein. Immunofluorescence should identify autophagosomes as LC3-positive and Lamp2-negative structures, because they have not yet fused with lysosomes. On the other hand, autolysosomes, which are hybrid organelles between autophagosomes and lysosomes, should be positive for both LC3 and Lamp2. Strikingly, the accumulated LC3 puncta in fed Rab7-KO cells were also positive for Lamp2 (Fig. 2C), and multiple LC3 puncta were often observed in swollen Lamp2-positive puncta (Fig. 2C, bottom panels, magnified views). The structures reminded us of yeast autophagic bodies, which are single membrane-bound vesicles containing a portion of cytoplasm in vacuoles lacking degradation activity (Takeshige et al., 1992).

Based on the above findings, we hypothesized that the autolysosomes in Rab7-KO cells decrease in size owing to

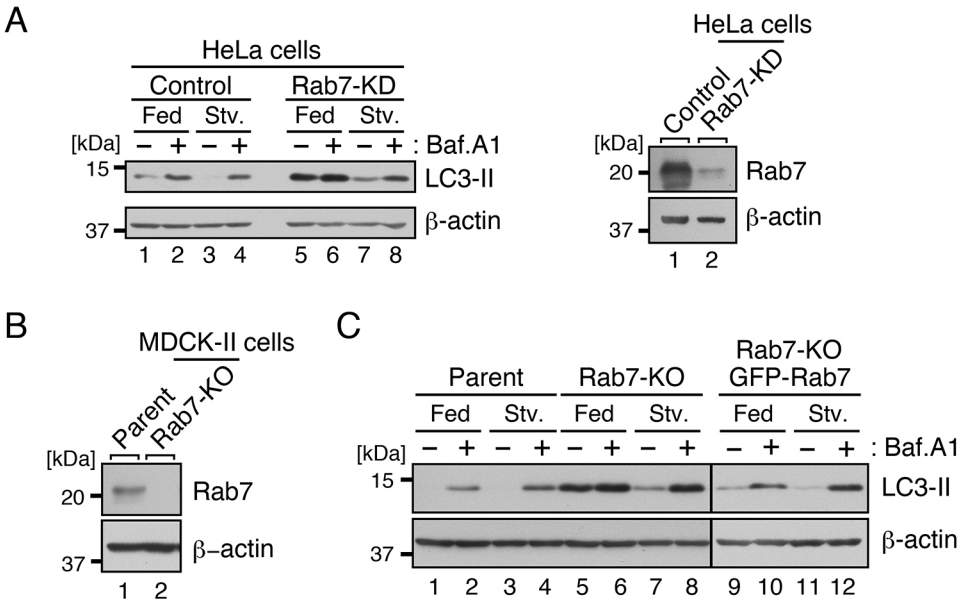

Fig. 1. Loss of Rab7 blocked LC3-II flux under fed conditions, but not under starved conditions. (A) LC3-II flux assays in Rab7-KD HeLa cells. HeLa cells were treated with control siRNA and siRNA against human Rab7. The cells were then cultured for 2 h in complete medium (Fed) or EBSS (Stv.) with or without 100 nM bafilomycin A1 (Baf.A1) and analyzed by immunoblotting with the antibodies indicated. The right panel shows the knockdown efficiency of *Rab7* siRNA. (B) Rab7-KO MDCK-II cells. Parental MDCK-II cells and Rab7-KO cells were homogenized and analyzed by immunoblotting with the antibodies indicated. (C) LC3-II flux assays in parental MDCK-II cells, Rab7-KO cells, and Rab7-KO cells stably expressing mouse GFP-Rab7 (Rab7-KO GFP-Rab7). The cells were cultured for 2 h in the complete medium (Fed) or EBSS (Stv.) with or without 100 nM bafilomycin A1 and analyzed by immunoblotting with the antibodies indicated. The positions of the molecular mass markers (in kDa) are shown on the left.

Journal of Cell Science (2018) 131, jcs215442. doi:10.1242/jcs.215442

degradation or maturation during nutrient starvation. To test this hypothesis, we measured the diameter of Lamp2-positive puncta in both fed and starved Rab7-KO cells, and as shown in Fig. 2D,E, the Rab7-KO cells were found to contain substantially larger Lamp2-positive puncta than the parental cells. Moreover, their puncta decreased in size during nutrient starvation. Live imaging of GFP–LC3 and Lamp1–mRFP in Rab7-KO cells confirmed the rapid maturation of LC3-positive autolysosomes during starvation (Fig. 2F; Fig. S1B, Movie 1). These results indicate that the autolysosomes that accumulate in Rab7-KO cells are cleared upon starvation.

To further verify the immunofluorescence findings described above, we performed a transmission electron microscope (TEM) analysis of parental and Rab7-KO cells. The high-electron-dense single-membrane structures in the electron micrographs are assumed to be autolysosomes or lysosomes, and consistent with the immunofluorescence findings, TEM revealed the presence of numerous electron-dense autolysosomes in the fed Rab7-KO cells (Fig. 3A, middle row, arrowheads). There were twice as many electron-dense structures in the fed Rab7-KO cells as in the parental cells (Fig. 3B). In contrast, hardly any autophagosomes, double-membrane-bound structures with intact cytosolic contents, were observed in the fed Rab7-KO cells (Fig. 3A). Consistent with the immunofluorescence findings, starvation of the Rab7-KO cells was followed by a clear decrease in the number of electron-dense structures (Fig. 3A,B). We therefore concluded that loss of Rab7 impairs autolysosome maturation under fed conditions alone.

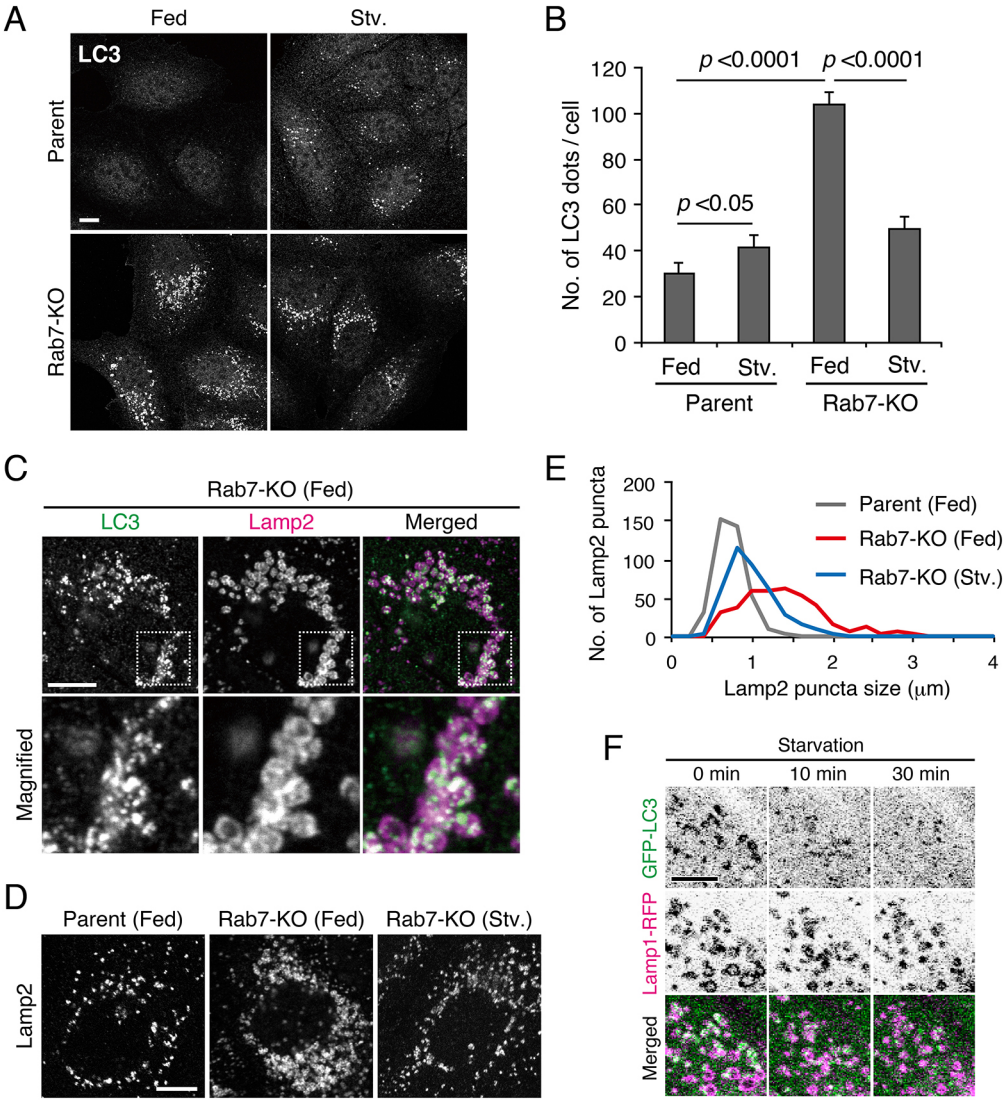

Fig. 2. Nutrient-starvation-induced clearance of accumulated autolysosomes in Rab7-KO cells. (A) Abnormal accumulation of LC3 puncta in MDCK-II cells under fed conditions. Parental and Rab7-KO cells were cultured for 2 h in complete medium (Fed) or EBSS (Stv.), and LC3 puncta were analyzed by means of immunofluorescence using a confocal fluorescence microscope. (B) Quantification of the number of LC3 puncta from 30 cells shown in A (mean±s.e.m.). (C) Accumulation of LC3- and Lamp2-positive autolysosomes in Rab7-KO cells. The cells were immunostained with anti-LC3 antibody (green) and anti-Lamp2 (lysosome marker; magenta) and analyzed with a confocal fluorescence microscope. Merged images are shown in the right column. The bottom panels are magnified views of the boxed areas in the top panels. (D) Rab7-KO cells contained significantly larger Lamp2-positive puncta than the parental cells, and the puncta decreased in size during nutrient starvation (see E). Parental and Rab7-KO cells were cultured for 2 h in the complete medium (Fed) or EBSS (Stv.), and Lamp2 puncta were analyzed by means of immunofluorescence using a confocal fluorescence microscope. (E) Histogram analysis of the diameters of Lamp2-positive puncta in parental cells (Fed), Rab7-KO cells (Fed) and Rab7-KO (Stv.) cells. 20 randomly selected puncta in each of 20 cells from each of the three groups were measured manually. (F) Time-lapse images of live-imaged starved Rab7-KO cells stably expressing GFP–LC3 and Lamp1–RFP. The time after the transfer to EBSS is indicated. Scale bars: 10 μm.

Journal of Cell Science (2018) 131, jcs215442. doi:10.1242/jcs.215442

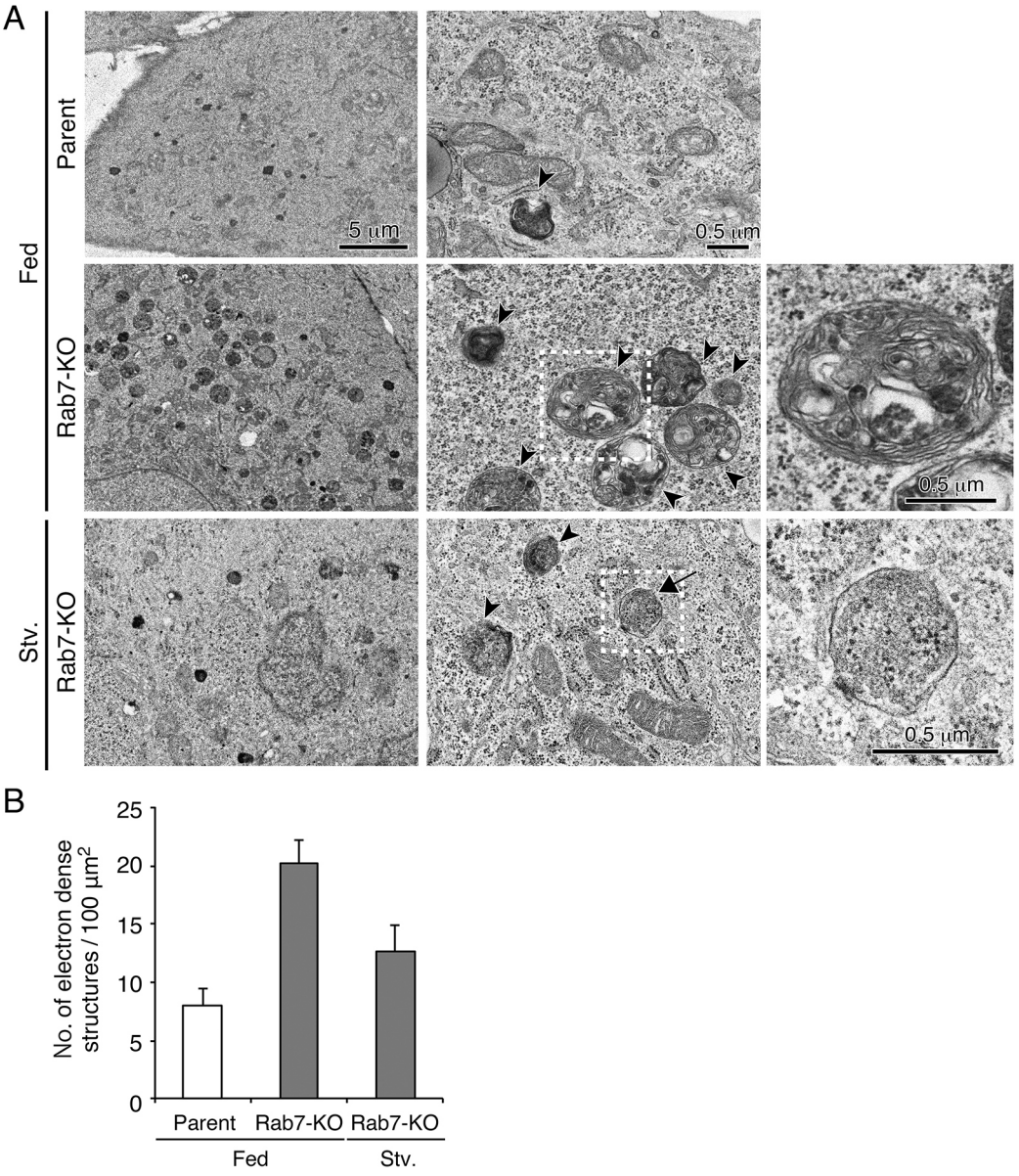

Fig. 3. Ultrastructure of the accumulated autolysosomes in fed Rab7-KO cells. (A) Typical TEM images of parental cells and Rab7-KO cells in complete medium (Fed) or EBSS (Stv.). The arrowheads point to autolysosomes or lysosomes, and the arrow points to an autophagosome. The right panels are magnified views of the boxed areas in the middle panels. (B) Quantification of the numbers of electron-dense structures (autolysosomes or lysosomes) in over 30 images (mean±s.e.m.).

mTORC1 inactivation is insufficient for starvation-induced clearance of autolysosomes

Although the accumulated LC3 puncta in Rab7-KO cells were cleared by starvation, a significant number of LC3 puncta remained after 2 h of starvation (Fig. 2A,B; Fig. 4A,B), and since starvation induces robust autophagosome formation, we hypothesized that newly formed autophagosomes were masking the starvation-induced clearance of autolysosomes in Rab7-KO cells. To test our hypothesis, we blocked autophagosome formation by exposing cells to wortmannin, a specific phosphoinositide 3-kinase (PI3K) inhibitor (Blommaart et al., 1997). As shown in Fig. 4A,B, wortmannin treatment significantly decreased the number of LC3 puncta under starved conditions, but not under fed conditions, indicating that the formation of new autophagosomes had actually masked the clearance of autolysosomes to some extent. We also performed a time-course experiment to measure the kinetics of LC3-II turnover in the presence of wortmannin. Rab7-KO cells were incubated in Earle's balanced salt solution (EBSS) containing wortmannin for various lengths of time, and LC3-II was detected by immunoblotting. The results revealed that the half-life of LC3-II in Rab7-KO cells was ∼10 min and that most of the accumulated LC3-II was degraded within 1 h after the start of starvation (Fig. 4C,D).

How does nutrient starvation induce autolysosome clearance in Rab7-KO cells? Since TFEB, a master regulator of lysosome homeostasis, has been reported to control expression of autophagy- and lysosome-related genes during starvation (Settembre et al., 2011; Peña-Llopis et al., 2011), we initially hypothesized that TFEB plays an important role in autolysosome clearance in Rab7-KO cells, and if it did, that the clearance mechanism would require transcription and translation of TFEB target genes. To determine

Journal of Cell Science (2018) 131, jcs215442. doi:10.1242/jcs.215442

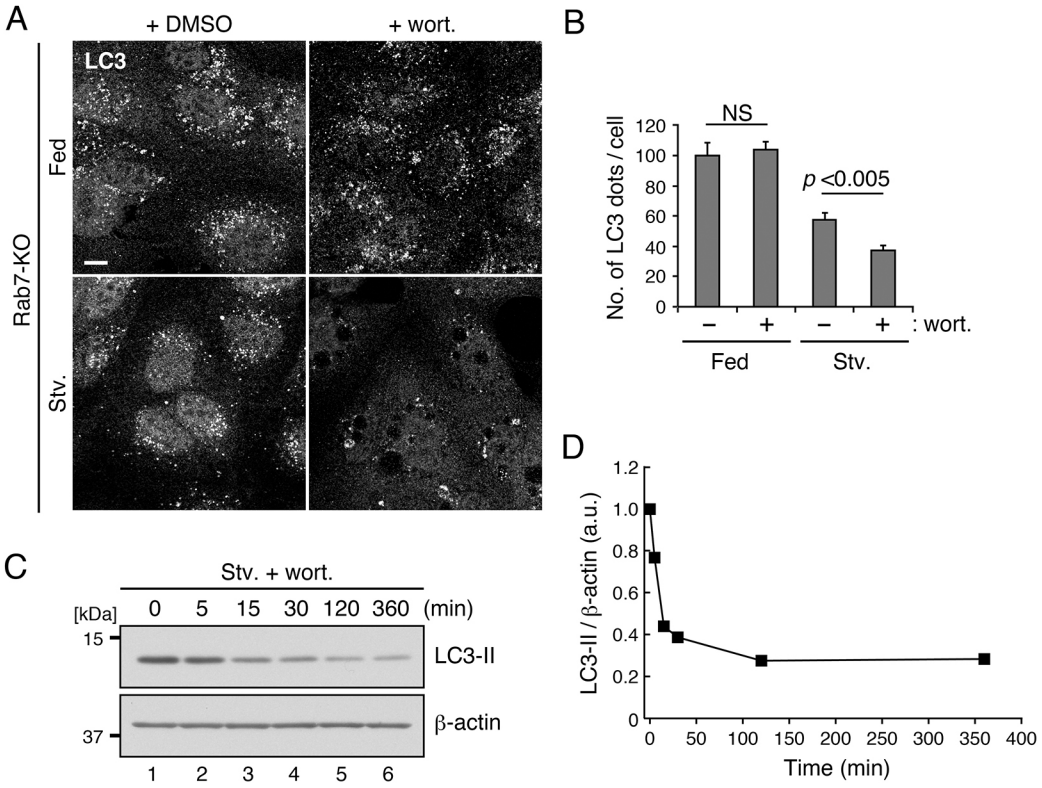

Fig. 4. Kinetics of the starvation-induced LC3-II turnover in Rab7-KO cells. (A) LC3-II flux assays in Rab7-KO MDCK-II cells incubated in the presence of wortmannin. Rab7-KO MDCK-II cells were cultured in complete medium for 2 days. The cells were then treated for 2 h in the complete medium (Fed) or EBSS (Stv.) with or without 200 nM wortmannin (wort.), and analyzed with a confocal fluorescence microscope. Scale bar: 10 µm. (B) Quantification of the number of LC3 puncta per cell in more than 30 cells from each group (mean±s.e.m.). NS, not significant. (C) Time course of LC3-II clearance after the start of starvation. Rab7-KO MDCK-II cells were incubated in EBSS (Stv.) in the presence of 200 nM wortmannin (wort.) for the times indicated and analyzed by immunoblotting with the antibodies indicated. The positions of the molecular mass markers (in kDa) are shown on the left. (D) Quantification of the level of LC3-II normalized to the β-actin levels for blots as shown in C.

whether newly synthesized proteins are required for autolysosome clearance, we treated Rab7-KO cells with a translation inhibitor, cycloheximide (CHX), and a transcription inhibitor, actinomycin D (ActD), but as shown in Fig. 5A, neither inhibitor blocked clearance of accumulated LC3-II in Rab7-KO cells, strongly suggesting that the starvation-induced autolysosome clearance is independent of transcription or translation.

Next, we investigated whether mechanistic/mammalian target of rapamycin complex 1 (mTORC1) is involved in the autolysosome clearance in Rab7-KO cells. mTORC1 is a central sensor of cellular energy status and regulates numerous pathways, including autophagy, through phosphorylation of target proteins (Zoncu et al., 2011). It is important to note that mTORC1-mediated mechanisms do not necessarily require transcription and translation, because, for example, mTORC1 negatively controls autophagy via direct phosphorylation of Atg13, a component of the ULK1/Atg1 complex (Hosokawa et al., 2009). We therefore hypothesized that inactivation of mTORC1 is crucial for autolysosome clearance in Rab7-KO cells. If our hypothesis was correct, treatment with an mTORC1 inhibitor should induce autolysosome clearance, the same as starvation does. Accordingly, we used Torin2, a specific inhibitor of mTORC1, to test our hypothesis. The results showed that both Torin2 and starvation almost completely blocked phosphorylation of S6 kinase (S6K) (P-S6K), which is a direct substrate of mTORC1 (Fig. 5B, second panel). To our surprise, however, Torin2 increased the level of LC3-II (Fig. 5B, top panel, and 5C), meaning that the effect of Torin2 on LC3-II flux was totally different from that of nutrient starvation. Torin2 is likely to robustly induce autophagy in Rab7-KO cells, but not autolysosome clearance. These results suggested that inactivation of mTORC1 is insufficient to induce autolysosome clearance in Rab7-KO cells.

Glutamine starvation induces autolysosome clearance in Rab7-KO cells

Since we used EBSS, which does not contain any amino acids, glucose or serum, to achieve nutrient starvation, the nutrient components required for autolysosome clearance were unknown. To identify the factor(s) essential for the starvation-induced autolysosome clearance, we incubated Rab7-KO cells in medium lacking individual amino acids, glucose (Glc) or serum (FBS, fetal bovine serum). As shown in Fig. 6A,B, amino acid starvation, but not glucose or serum starvation, significantly induced clearance of accumulated LC3-II in Rab7-KO cells, essentially the same as incubation in EBSS did. This finding suggested that amino acid depletion is the key trigger for autolysosome clearance.

Since standard growth medium (Dulbecco's modified Eagle's medium; DMEM) for cultured cells contains 15 amino acids (Arg, Cys, Gln, Gly, His, Ile, Leu, Lys, Met, Phe, Ser, Thr, Trp, Tyr and Val), we next attempted to identify the amino acid(s) involved in the induction of the autolysosome clearance by incubating Rab7-KO cells in medium containing all 15 amino acids simultaneously and containing each one of them individually. Strikingly, addition of glutamine alone to amino-acid-free medium clearly blocked the clearance of LC3-II (Fig. 6C, lane 6), essentially the same as

Journal of Cell Science (2018) 131, jcs215442. doi:10.1242/jcs.215442

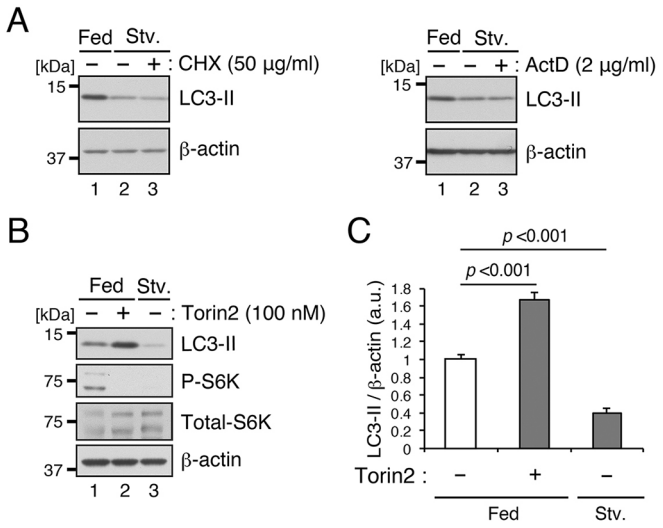

Fig. 5. mTORC1 inactivation is insufficient for starvation-induced autolysosome clearance. (A) Effect of cycloheximide and actinomycin D on starvation-induced LC3-II clearance. Rab7-KO MDCK-II cells were cultured in complete medium for 2 days. The cells were then incubated for 2 h in the complete medium (Fed) or EBSS (Stv.) with or without 50 μg/ml cycloheximide (CHX; translation inhibitor; left panel) or 2 μg/ml actinomycin D (ActD; transcription inhibitor; right panel), and analyzed by immunoblotting with the antibodies indicated. (B) Effect of Torin2 on starvation-induced LC3-II clearance. Rab7-KO MDCK-II cells were cultured in the complete medium for 2 days. The cells were then incubated for 2 h in the complete medium (Fed) or EBSS (Stv.) with or without 100 nM Torin2 (a specific mTORC1 inhibitor), and analyzed by immunoblotting with the antibodies indicated. The positions of the molecular mass markers (in kDa) are shown on the left in A and B. (C) Quantification of the level of LC3-II normalized to the β-actin levels for blots as shown in B (mean±s.e.m.; *n*=3).

addition of all 15 amino acids did (Fig. 6C, lane 3), indicating that glutamine is the critical amino acid for autolysosome clearance. It should be noted that addition of none of the other 14 amino acids affected LC3-II turnover (Fig. 6C). We investigated whether depletion of glutamine alone would also induce autolysosome clearance, and, as expected, depletion of glutamine alone resulted in a dramatic decrease in the LC3-II level, and replenishment to 4 mM glutamine blocked LC3-II turnover (Fig. 6D,E). We also confirmed that the LC3 puncta that accumulated in fed Rab7-KO cells were cleared upon glutamine starvation (Fig. 6F,G). These results indicated that glutamine is the critical factor for the autolysosome clearance in Rab7-KO cells.

Glutamine starvation induces autolysosome clearance even in the presence of Rab7

Finally, we investigated whether the autolysosome clearance phenomenon, which was originally found in Rab7-KO cells, occurs even in the presence of Rab7. Rab7-KO cells stably expressing exogenous Rab7 (Rab7-rescued cells) were incubated with or without glutamine and immunostained for LC3 and Lamp2. Rab7-rescued cells contained a moderate number of LC3 puncta under fed conditions (Fig. 7A, top panel) similarly to parental wild-type cells, and, importantly, these LC3 puncta often colocalized well with Lamp2, indicating that autolysosomes are actually present in fed Rab7-rescued cells (Fig. 7A, top panel, insets). Glutamine starvation resulted in a significant decrease in the number of LC3 puncta (Fig. 7A,B). Consistent with the immunofluorescence findings, glutamine starvation also resulted in a decrease in the LC3-II level in Rab7-rescued cells (Fig. 7C). To assess whether it might be possible to generalize these findings, we also starved wild-type HeLa cells for glutamine, and once again the results showed that the LC3-positive autolysosomes were almost completely cleared upon glutamine starvation (Fig. 7D,E; Fig. S2). These findings suggested that glutamine starvation induces autolysosome clearance irrespective of the presence of Rab7. Taken together, our results for the first time demonstrate that nutrient starvation regulates a very late stage of autophagy, namely, autolysosome maturation.

DISCUSSION

In the present study, we re-investigated the function of Rab7 in autophagy by using Rab7-KO cells and the results yielded two unexpected findings. The first unexpected finding in this study was that Rab7 is dispensable for fusion between autophagosomes and lysosomes in mammalian cells: a significant number of autolysosomes, but not autophagosomes, accumulated in fed Rab7-KO cells (Figs 2 and 3). In sharp contrast, Ypt7/Rab7 in yeast and flies functions in the autophagosome–vacuole/lysosome fusion step, and autophagosomes accumulate in Ypt7/Rab7-deficient cells (Kirisako et al., 1999; Fujita et al., 2017; Hegedűs et al., 2016). Consequently, the function of Rab7 in autophagy may have changed or a backup mechanism may have developed during the course of evolution. One possible backup mechanism is compensation by other Rab isoforms, because mammals contain Rab7b (also called Rab42), which is distantly related to Rab7 (Fukuda, 2010). However, Rab7b is most unlikely to be involved in the process of autophagy, because Rab7b-KO cells exhibited normal autophagy flux (Fig. S3A) and both Rab7-KD cells and Rab7-KD/Rab7b-KO cells showed essentially the same autolysosome accumulation phenotype (Fig. S3B).

Although mammalian Rab7 is not essential for fusion between autophagosomes and lysosomes, it is still possible that Rab7 functions in fusion events. Two possible scenarios explain the Rab7-KO phenotype under fed conditions. The first possible scenario is that Rab7 functions in the amphisome–lysosome fusion step (Jäger et al., 2004). It has been proposed that autophagosomes sequentially fuse with endosomes and lysosomes to form amphisomes and autolysosomes, respectively (Shen and Mizushima, 2014; Nakamura and Yoshimori, 2017). If loss of Rab7 specifically blocks amphisome–lysosome fusion, then amphisomes, which are partially degraded intermediates, would accumulate in Rab7-KO cells. It should be noted that the electron-dense structures that accumulated in fed Rab7-KO cells often contained membranous structures, the same as amphisomes do (Fig. 3A), and thus it is possible that Rab7 contributes to amphisome–lysosome fusion. The second possible scenario is that Rab7 regulates the efficiency of autophagosome–lysosome fusion. It has recently been shown that, in mammals, a single autophagosome fuses with multiple lysosomes, thereby ensuring complete degradation of its contents (Yu et al., 2010; Tsuboyama et al., 2016). Rab7 may promote fusion between an autophagosome and a limited number of lysosomes, and an additional fusion factor(s) must be required for fusion with additional lysosomes. In the absence of Rab7, the autophagosome would be unable to fuse with a sufficient number of lysosomes and autolysosomes would accumulate. If such additional fusion factors are activated by starvation, starvation-induced clearance of autolysosomes in Rab7-KO cells (see next section) would be explained by additional fusion with lysosomes. However, we do not favor this scenario, because our live imaging data showed that autolysosomes shrank without fusing with additional lysosomes (Movie 1).

Journal of Cell Science (2018) 131, jcs215442. doi:10.1242/jcs.215442

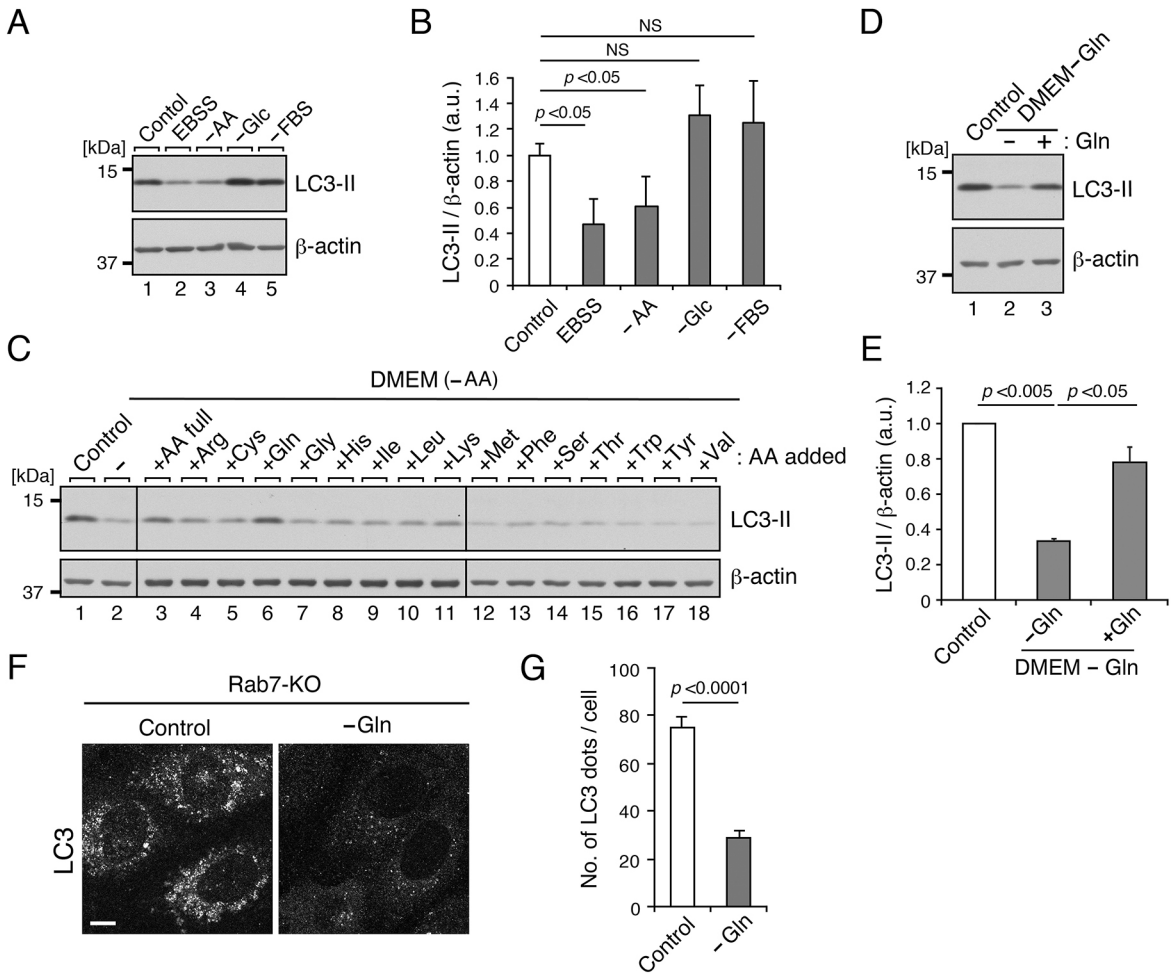

Fig. 6. Glutamine-starvation-induced autolysosome clearance in Rab7-KO cells. (A) LC3-II clearance in Rab7-KO cells depends on amino acids (AA), but not on glucose (Glc) or on FBS. Rab7-KO MDCK-II cells were cultured in complete medium for 2 days. The cells were then incubated for 2 h in either the complete medium (control), EBSS, DMEM (–AA), DMEM (–Glc) or DMEM (–FBS), and analyzed by immunoblotting with the antibodies indicated. (B) Quantification of the level of LC3-II normalized to the β-actin levels for blots as shown in A (mean±s.e.m.; *n*=3). NS, not significant. (C) LC3-II clearance in Rab7-KO cells depends on Gln. Rab7-KO MDCK-II cells were cultured in the complete medium for 2 days. The cells were then incubated for 2 h in either the complete medium (control), DMEM (–AA) or DMEM (–AA) containing the amino acids indicated, and were analyzed by immunoblotting with the antibodies indicated. (D) Rab7-KO MDCK-II cells were cultured in the complete medium for 2 days. The cells were then incubated for 2 h in either the complete medium (control), DMEM (–Gln) or DMEM (–Gln) containing 4 mM glutamine and analyzed by immunoblotting with the antibodies indicated. The positions of the molecular mass markers (in kDa) are shown on the left in A, C and D. (E) Quantification of the level of LC3-II normalized to the β-actin levels for blots as shown in D (mean±s.e.m.; *n*=3). (F) Gln-starvation-induced clearance of LC3 puncta in Rab7-KO MDCK-II cells. The cells were cultured as described in D, and immunostained with the antibodies indicated. Scale bar: 10 µm. (G) Quantification of the number of LC3 puncta in 30 cells shown in F (mean±s.e.m.).

The second unexpected finding in this study was that the autolysosomes that had accumulated in fed Rab7-KO cells were quickly and specifically cleared upon glutamine starvation (Figs 4 and 6): nutrient starvation promoted autolysosome maturation in Rab7-KO cells in addition to promoting autophagosome formation. More importantly, glutamine-starvation-induced autolysosome maturation was also observed in wild-type cells, indicating that it occurs irrespective of the presence or absence of Rab7 (Fig. 7). The precise molecular mechanism by which glutamine promotes autolysosome maturation is unknown, and it will need to be identified in a future study. We suggest two possible mechanisms that would explain starvation-induced autolysosome maturation. The first possible mechanism is one mediated by TFEB, which regulates expression of myriad genes required for lysosome homeostasis (Settembre et al., 2011; Peña-Llopis et al., 2011; Vega-Rubin-de-Celis et al., 2017). However, such a mechanism is highly unlikely because of the following two findings: (1) neither a transcription inhibitor nor a translation inhibitor blocked starvation-induced autolysosome clearance in Rab7-KO cells (Fig. 5A), and (2) Torin2-mediated inactivation of mTORC1 failed to induce autolysosome clearance (Fig. 5B,C) despite the fact that mTORC1 negatively regulates TFEB by means of phosphorylation of TFEB. The second possible, and more likely, mechanism is regulation of V-ATPase assembly. The V-ATPase consists of two subcomplexes, a peripheral subcomplex (V_1) that comprises the ATP-binding sites and an integral membrane subcomplex (V_0) that forms the proton pore, and assembly of the V_0 subcomplex and V_1 subcomplex has been shown to be reversibly controlled by starvation (Stransky and Forgac, 2015). In addition, other studies have shown that starvation boosts lysosomal acidification (Ni et al., 2011; Zhou et al., 2013). If lysosomal acidification is partially attenuated by loss of Rab7, starvation would promote autolysosome maturation through this mechanism, and a Rab7 effector, RILP, has actually been shown to regulate V-ATPase

Journal of Cell Science (2018) 131, jcs215442. doi:10.1242/jcs.215442

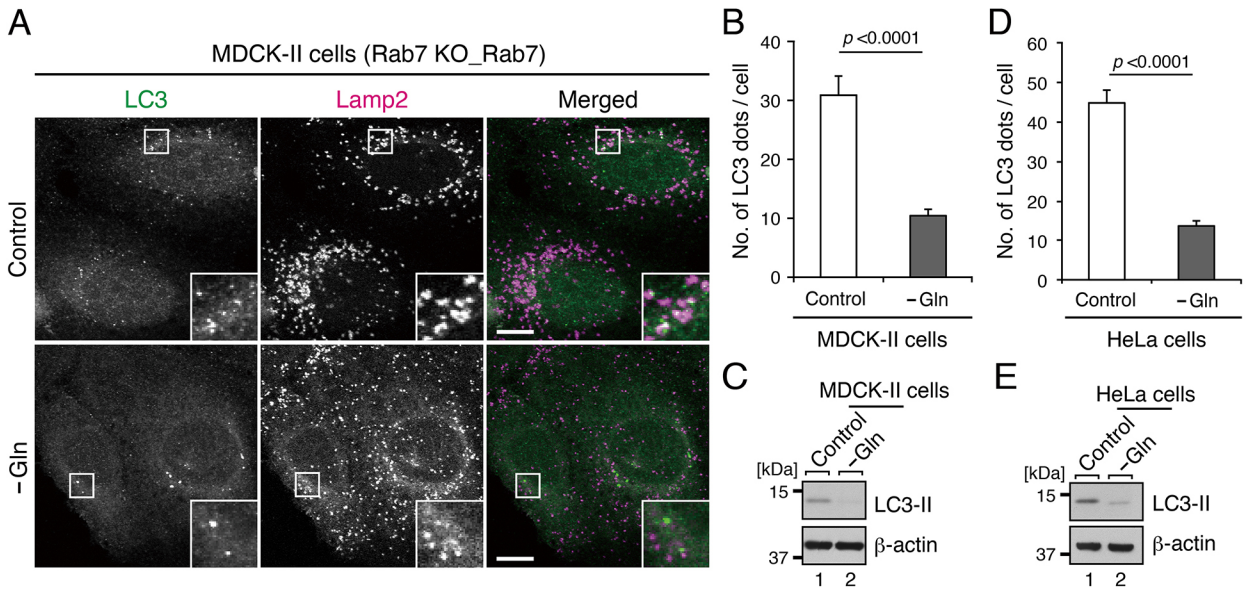

Fig. 7. Glutamine starvation induced autolysosome clearance even in the presence of Rab7. (A) Gln-starvation-induced clearance of LC3 puncta in MDCK-II cells. MDCK-II cells (Rab7-KO cells stably expressing Rab7) were cultured in the complete medium for 2 days. The cells were then incubated for 2 h in complete medium (control) or DMEM (–Gln), immunostained with anti-LC3 antibody (green) and anti-Lamp2 (lysosome marker; magenta), and analyzed with a confocal fluorescence microscope. (B) Quantification of the number of LC3 puncta per cell in more than 10 cells from each group (mean±s.e.m.). (C) Gln-starvation-induced clearance of LC3-II in MDCK-II cells. MDCK-II cells (Rab7-KO cells stably expressing Rab7) were cultured as in A, and then analyzed by immunoblotting with the antibodies indicated. (D) Gln-starvation-induced clearance of LC3 puncta in HeLa cells. HeLa cells were also cultured as in A, and the number of LC3 puncta per cell in more than 30 cells from each treatment group was quantified (mean±s.e.m.). (E) Gln-starvation-induced clearance of LC3-II in HeLa cells. HeLa cells were also cultured as in A, and analyzed by immunoblotting with the antibodies indicated. The positions of the molecular mass markers (in kDa) are shown on the left in C and E.

through interaction with its V1G1 subunit (De Luca et al., 2014). Thus, it is tempting to speculate that the autolysosome accumulation in fed Rab7-KO cells is caused by lysosomal dysfunction (i.e. by incomplete lysosome acidification) and that glutamine starvation promotes V-ATPase assembly through a Rab7-independent mechanism. So far as we tested, however, we did not detect any significant defects in lysosomal pH (as monitored by LysoTracker) or acid protease activity (as monitored by Magic Red) as a result of loss of Rab7 (Fig. S4A). Although the cathepsin B activity in Rab7-KO cells was still observed when monitored by Magic Red, we also found that the amount of a mature form of cathepsin B was clearly reduced in Rab7-KO cells (Fig. S4B), indicating that Rab7 is partly involved in processing or targeting of certain lysosomal enzymes to lysosomes. Therefore, it is highly possible that acid protease activity of certain lysosomal enzymes is reduced in Rab7-KO cells. Extensive future research will be necessary to determine whether lysosomal functions in Rab7-KO cells are actually impaired under fed conditions.

Why glutamine and none of the other amino acids play a central role in starvation-induced autolysosome maturation (Figs 6 and 7) is another important open question that needs to be answered in a future study. Glutamine is the most abundant amino acid in mammalian cells and is known to be a crucial intracellular energy source (Curi et al., 2005). In that sense, it is not surprising that cells monitor their glutamine level to regulate autophagy. Autophagosome formation has been reported to be regulated by the glutamine level through mTORC1 inactivation (Chen et al., 2014; Tan et al., 2017; Durán et al., 2012). Glutamine is metabolized through glutaminolysis to produce α-ketoglutarate, which regulates Rag GTPase, a positive regulator of mTORC1 (Durán et al., 2012). However, since glutamine-starvation-induced autolysosome maturation appears to occur independently of mTORC1 (Fig. 5B,C), at least two different glutamine-sensing mechanisms, that is, an mTORC1-dependent mechanism and an mTORC1-independent mechanism, must exist in cells to regulate different steps of autophagy.

In conclusion, in this study we demonstrate that unlike what is seen with fly Rab7 and yeast Ypt7, mammalian Rab7 is not essential for the fusion between autophagosomes and lysosomes, and that autolysosomes accumulate in Rab7-KO cells only under fed conditions. We also discovered a novel phenomenon: glutamine-starvation-induced maturation of autolysosomes both in wild-type cells and in Rab7-KO cells, where the phenomenon was emphasized because of autolysosome accumulation under fed conditions. Thus, the Rab7-KO cells established in this study will open new avenues for studying the molecular mechanism underlying glutamine-starvation-induced autolysosome maturation.

MATERIALS AND METHODS

Materials

Bafilomycin A1 and actinomycin D were obtained from Sigma-Aldrich (St Louis, MO). Cycloheximide, wortmannin and Torin2 were purchased from Wako Pure Chemical Industries, Ltd. (Osaka, Japan), Cell Signaling Technology (Danvers, MA) and Abcam (Tokyo, Japan), respectively. The following commercially available antibodies were used in this study: anti-LC3 rabbit polyclonal antibody (MBL, Nagoya, Japan), anti-β-actin mouse monoclonal antibody (Applied Biological Materials, Richmond, British Columbia, Canada), anti-Rab7 rabbit monoclonal antibody, anti-S6 kinase (S6K) rabbit polyclonal antibody, anti-phospho-p70-S6 kinase (Thr389) rabbit polyclonal antibody (Cell Signaling Technology), anti-Lamp2 mouse monoclonal antibody (MA5-16561; Thermo Fisher Scientific Corp., Waltham, MA), and anti-cathepsin B mouse monoclonal antibody (sc-365558; Santa Cruz Biotechnology). All other reagents used in this study were analytical grade or the highest grade commercially available.

Journal of Cell Science (2018) 131, jcs215442. doi:10.1242/jcs.215442

Plasmid construction

pMRX-IRES-puro-EGFP-LC3 was prepared as described previously (Itoh et al., 2011). cDNA encoding the mouse Rab7 (Kuroda et al., 2002) was subcloned into the pMRX-puro vector and pMRX-puro-EGFP vector (Saitoh et al., 2003). pMRX-puro-EGFP and pMRX-IRES-bsr-Lamp1-RFP were kind gifts from Dr Shoji Yamaoka (Tokyo Medical and Dental University, Tokyo, Japan) and Dr Tamotsu Yoshimori (Osaka University, Osaka, Japan), respectively.

Cell culture and drug exposure

MDCK-II cells and HeLa cells were grown at 37°C in DMEM (Wako Pure Chemical Industries, Ltd.) supplemented with 10% fetal bovine serum (FBS), 100 units/ml penicillin G and 100 µg/ml streptomycin (complete medium) in a 5% CO_2 incubator. Plat-E cells were a kind gift from Dr Toshio Kitamura (The University of Tokyo, Tokyo, Japan) and they were cultured in the same complete medium as the MDCK-II cells and HeLa cells. Retrovirus production in Plat-E cells and retrovirus infection were performed as described previously (Morita et al., 2000). Stable transformants of MDCK-II Rab7-KO cells expressing EGFP–Rab7 or Rab7 were selected in the complete medium by exposing them to 2 µg/ml puromycin (Thermo Fisher Scientific Corp.) for 24–48 h.

The starvation procedure was as follows. At 2 days after replating MDCK-II cells and HeLa cells in the complete medium, the cells were quickly rinsed once with PBS and then incubated for 2 h in either EBSS, DMEM containing no glutamine (–Gln), DMEM without FBS (–FBS), DMEM without amino acids (–AA), or DMEM without glucose (–Glc) (Wako Pure Chemical Industries, Ltd.). The amino acid addition experiments were performed by incubating MDCK-II cells in DMEM (–Gln) and 4 mM Gln or in DMEM (–AA) plus one of the following amino acids: 84 µg/l Arg, 62.6 µg/l Cys (cystin-2HCl), 584 µg/l (4 mM) Gln, 30 µg/l Gly, 42 µg/l His, 105 µg/l Ile, 105 µg/l Leu, 146 µg/l Lys, 30 µg/l Met, 66 µg/l Phe, 42 µg/l Ser, 95 µg/l Thr, 16 µg/l Trp, 103.79 µg/l Tyr (Tyr-2Na-2H_2O), and 94 µg/l Val. Cells were also exposed for 2 h to 200 nM wortmannin, 50 µg/ml cycloheximide, or 2 µg/ml actinomycin D under starved conditions.

siRNA-mediated Rab7 knockdown in HeLa cells and CRISPR/Cas9-mediated Rab7 KO in MDCK-II cells

An siRNA against human Rab7 (target sequence: 5′-GGAGCTGACTTTCTGACCA-3′; Aizawa and Fukuda, 2015) was transfected into HeLa cells by using Lipofectamine RNAiMAX (Thermo Fisher Scientific Corp.) according to the manufacturer's instructions. The CRISPR/Cas9-mediated Rab7 knockout [single guide RNA (sgRNA) target sequence: 5′-GGAACGGTTCCAGTCCCTTG-3′] in MDCK-II cells was performed as described previously (Mrozowska and Fukuda, 2016), by using pSpCas9 (BB) 2A-Puro vector (Addgene, Cambridge, MA). In brief, pSpCas9-Rab7-KO plasmids were transfected into parental (wild-type) MDCK-II cells by using Lipofectamine 2000 (Thermo Fisher Scientific Corp.) according to the manufacturer's instructions. After 1 day, the transfected cells were selected by exposure to 2 µg/ml puromycin. Then, 2 days later the cells were trypsinized and cloned by limited dilution. Clonal lines were isolated and analyzed by immunoblotting with specific anti-Rab7 antibody to determine the endogenous Rab7 protein level. *Rab7* gene knockout was confirmed by sequencing genomic DNA.

Immunoblotting

Equal amounts of proteins per sample were subjected to 12.5% SDS-PAGE, and transferred to polyvinylidene difluoride membranes. The membranes were blocked with PBS-T (PBS and 0.1% Tween 20) containing 1% skimmed milk and incubated for 1 h at 4°C with primary antibodies (1:1000–1:5000 dilution in the blocking solution; Table S1). The membranes were washed three times with PBS-T and then incubated for 30 min at room temperature with appropriate horseradish peroxidase (HRP)-conjugated secondary antibodies in the blocking solution. After washing the membranes three times with PBS-T, immunoreactive bands were detected with enhanced chemiluminescence and X-ray films.

Immunofluorescence analysis

For the immunofluorescence analysis, cells were cultured on coverslips, fixed with 4% paraformaldehyde in PBS for 10 min, and permeabilized with 50 µg/ml digitonin in PBS for 5 min. The cells were then blocked with PBS containing 0.1% gelatin for 10 min. The coverslips were first incubated for 1 h at room temperature with primary antibodies (1:1000 dilution in PBS containing 0.1% gelatin), washed five times with PBS, and then incubated for 45 min with appropriate Alexa Fluor-conjugated secondary antibodies (Thermo Fisher Scientific Corp.). The samples were mounted using ProLong Gold Antifade Mountant (Thermo Fisher Scientific Corp.). The immunostained samples were analyzed by using a FV1000D confocal fluorescence microscope with a 60× oil/1.4 NA Plan Apochromatic objective lens and Fluoview software (Olympus, Tokyo, Japan). The images acquired were processed with Photoshop CS6 (Adobe, San Jose, CA) and ImageJ software (version 1.49; National Institutes of Health; available at https://imagej.nih.gov/ij/). Quantification of LC3 puncta was performed using ImageJ as previously described (Itoh et al., 2011).

Live-cell imaging

Live-cell fluorescence imaging was performed by using a FV1000D confocal fluorescence microscope with a 60× oil/1.4 NA Plan Apochromatic objective lens and Fluoview software. Cells stably expressing marker proteins fused to GFP or RFP variants were placed on a 35-mm glass bottom dish (MatTek, Ashland, MA) 1 day before imaging. During live-cell imaging, the dish was mounted in a chamber (INUB-ONI-F2; Tokai Hit. Co., Ltd., Shizuoka, Japan) to maintain incubation conditions at 37°C and 5% CO_2. Images were acquired at intervals of 1 min and analyzed with ImageJ.

Electron microscopy

For the TEM analysis, cells grown in the complete medium for 2 days were cultured for 2 h in either fresh complete medium or EBSS for 2 h. The cells were then fixed for 30 min at 4°C with 2% paraformaldehyde and 2% glutaraldehyde in 0.1 M phosphate buffer (pH 7.4). The samples were then dehydrated in a graded series of ethanol solutions: in a 50% solution at 4°C, and a 70% solution at 4°C for 5 min each, in a 90% solution for 5 min at room temperature, and then three times in a fresh 100% solution for 5 min each time at room temperature. For embedding and polymerization, the samples were transferred to a resin (Quatol-812; Nisshin EM Co., Tokyo, Japan) and polymerized at 60°C for 48 h. The polymerized resins were ultra-thin sectioned at 70 nm with a diamond knife, using an ultramicrotome (Ultra cut UCT; Leica, Vienna, Austria), and the sections were mounted on copper grids. The sections were stained with 2% uranyl acetate at room temperature for 15 min, and then washed with distilled water followed by being secondarily stained for 3 min with lead stain solution (Sigma-Aldrich Co.) at room temperature. The sections were examined with a transmission electron microscope (JEM-1400 Plus; JEOL Ltd., Tokyo, Japan) at an acceleration voltage of 80 kV. Digital images (3296×2472 pixels) were taken with a CCD camera (CEM-14830 RUBY 2; JEOL Ltd.). The above protocols were provided by Tokai Electron Microscopy, Inc. (Aichi, Japan).

Statistical analysis

The data were statistically analyzed by performing Student's unpaired *t*-test with Bonferroni multiple correction. All values in the figures are shown as the mean±s.d. or mean±s.e.m. P values <0.05 were considered statistically significant.

Acknowledgements

We thank Drs Tamotsu Yoshimori, Toshio Kitamura and Shoji Yamaoka for kindly donating materials, Megumi Aizawa for technical assistance, and members of the Fukuda laboratory for valuable discussions.

Competing interests

The authors declare no competing or financial interests.

Author contributions

Conceptualization: Y.K., N.F., M.F.; Methodology: Y.K., N.F.; Validation: Y.K., N.F., M.F.; Investigation: Y.K.; Resources: M.F.; Data curation: Y.K.; Writing - original draft:

Y.K., N.F., M.F.; Writing - review & editing: Y.H., N.F., M.F.; Project administration: N.F., M.F.; Funding acquisition: Y.H., M.F.

Funding

This work was supported in part by Grant-in-Aid for Scientific Research(B) from the Ministry of Education, Culture, Sports, Science and Technology (MEXT) of Japan (grant number 15H04367 to M.F.), Grants-in-Aid for Scientific Research on Innovative Areas from MEXT (grant numbers 16H01189 and 17H05682 to M.F.), by the Japan Science and Technology Agency (JST) CREST (grant number JPMJCR17H4 to M.F.), and by the Japan Society for the Promotion of Science (to Y.H.).

Supplementary information

Supplementary information available online at
http://jcs.biologists.org/lookup/doi/10.1242/jcs.215442.supplemental

References

Aizawa, M. and Fukuda, M. (2015). Small GTPase Rab2B and its specific binding protein Golgi-associated Rab2B interactor-like 4 (GARI-L4) regulate Golgi morphology. *J. Biol. Chem.* **290**, 22250-22261.

Ao, X., Zou, L. and Wu, Y. (2014). Regulation of autophagy by the Rab GTPase network. *Cell Death Differ.* **21**, 348-358.

Blommaart, E. F. C., Krause, U., Schellens, J. P. M., Vreeling-Sindelárová, H. and Meijer, A. J. (1997). The phosphatidylinositol 3-kinase inhibitors wortmannin and LY294002 inhibit autophagy in isolated rat hepatocytes. *Eur. J. Biochem.* **243**, 240-246.

Bucci, C., Thomsen, P., Nicoziani, P., McCarthy, J. and van Deurs, B. (2000). Rab7: a key to lysosome biogenesis. *Mol. Biol. Cell* **11**, 467-480.

Chen, R., Zou, Y., Mao, D., Sun, D., Gao, G., Shi, J., Liu, X., Zhu, C., Yang, M., Ye, W. et al. (2014). The general amino acid control pathway regulates mTOR and autophagy during serum/glutamine starvation. *J. Cell Biol.* **206**, 173-182.

Curi, R., Lagranha, C. J., Doi, S. Q., Sellitti, D. F., Procopio, J., Pithon-Curi, T. C., Corless, M. and Newsholme, P. (2005). Molecular mechanisms of glutamine action. *J. Cell. Physiol.* **204**, 392-401.

De Luca, M., Cogli, L., Progida, C., Nisi, V., Pascolutti, R., Sigismund, S., Di Fiore, P. P. and Bucci, C. (2014). RILP regulates vacuolar ATPase through interaction with the V1G1 subunit. *J. Cell Sci.* **127**, 2697-2708.

Durán, R. V., Oppliger, W., Robitaille, A. M., Heiserich, L., Skendaj, R., Gottlieb, E. and Hall, M. N. (2012). Glutaminolysis activates Rag-mTORC1 signaling. *Mol. Cell* **47**, 349-358.

Fujita, N., Huang, W., Lin, T.-H., Groulx, J.-F., Jean, S., Nguyen, J., Kuchitsu, Y., Koyama-Honda, I., Mizushima, N., Fukuda, M. et al. (2017). Genetic screen in Drosophila muscle identifies autophagy-mediated T-tubule remodeling and a Rab2 role in autophagy. *eLife* **6**, e23367.

Fukuda, M. (2008). Membrane traffic in the secretory pathway: regulation of secretory vesicle traffic by Rab small GTPases. *Cell. Mol. Life Sci.* **65**, 2801-2813.

Fukuda, M. (2010). How can mammalian Rab small GTPases be comprehensively analyzed?: development of new tools to comprehensively analyze mammalian Rabs in membrane traffic. *Histol. Histopathol.* **25**, 1473-1480.

Fukuda, M. and Itoh, T. (2008). Direct link between Atg protein and small GTPase Rab: Atg16L functions as a potential Rab33 effector in mammals. *Autophagy* **4**, 824-826.

Guerra, F. and Bucci, C. (2016). Multiple roles of the small GTPase Rab7. *Cells* **5**, 34.

Gutierrez, M. G., Munafó, D. B., Berón, W. and Colombo, M. I. (2004). Rab7 is required for the normal progression of the autophagic pathway in mammalian cells. *J. Cell Sci.* **117**, 2687-2697.

Hegedűs, K., Takáts, S., Boda, A., Jipa, A., Nagy, P., Varga, K., Kovács, A. L. and Juhász, G. (2016). The Ccz1-Mon1-Rab7 module and Rab5 control distinct steps of autophagy. *Mol. Biol. Cell* **27**, 3132-3142.

Hosokawa, N., Hara, T., Kaizuka, T., Kishi, C., Takamura, A., Miura, Y., Iemura, S.-I., Natsume, T., Takehana, K., Yamada, N. et al. (2009). Nutrient-dependent mTORC1 association with the ULK1-Atg13-FIP200 complex required for autophagy. *Mol. Biol. Cell* **20**, 1981-1991.

Hutagalung, A. H. and Novick, P. J. (2011). Role of Rab GTPases in membrane traffic and cell physiology. *Physiol. Rev.* **91**, 119-149.

Hyttinen, J. M. T., Niittykoski, M., Salminen, A. and Kaarniranta, K. (2013). Maturation of autophagosomes and endosomes: a key role for Rab7. *Biochim. Biophys. Acta Mol. Cell Res.* **1833**, 503-510.

Itoh, T., Kanno, E., Uemura, T., Waguri, S. and Fukuda, M. (2011). OATL1, a novel autophagosome-resident Rab33B-GAP, regulates autophagosomal maturation. *J. Cell Biol.* **192**, 839-853.

Jäger, S., Bucci, C., Tanida, I., Ueno, T., Kominami, E., Saftig, P. and Eskelinen, E. L. (2004). Role for Rab7 in maturation of late autophagic vacuoles. *J. Cell Sci.* **117**, 4837-4848.

Jean, S. and Kiger, A. A. (2012). Coordination between RAB GTPase and phosphoinositide regulation and functions. *Nat. Rev. Mol. Cell Biol.* **13**, 463-470.

Kabeya, Y., Mizushima, N., Ueno, T., Yamamoto, A., Kirisako, T., Noda, T., Kominami, E., Ohsumi, Y. and Yoshimori, T. (2000). LC3, a mammalian homologue of yeast Apg8p, is localized in autophagosome membranes after processing. *EMBO J.* **19**, 5720-5728.

Kirisako, T., Baba, M., Ishihara, N., Miyazawa, K., Ohsumi, M., Yoshimori, T., Noda, T. and Ohsumi, Y. (1999). Formation process of autophagosome is traced with Apg8/Aut7p in yeast. *J. Cell Biol.* **147**, 435-446.

Klionsky, D. J., Abdelmohsen, K., Abe, A., Abedin, M. J., Abeliovich, H., Acevedo Arozena, A., Adachi, H., Adams, C. M., Adams, P. D., Adeli, K. et al. (2016). Guidelines for the use and interpretation of assays for monitoring autophagy (3rd edition). *Autophagy* **12**, 1-222.

Kuroda, T. S., Fukuda, M., Ariga, H. and Mikoshiba, K. (2002). The Slp homology domain of synaptotagmin-like proteins 1-4 and Slac2 functions as a novel Rab27A binding domain. *J. Biol. Chem.* **277**, 9212-9218.

Lőrincz, P., Tóth, S., Benkő, P., Lakatos, Z., Boda, A., Glatz, G., Zobel, M., Bisi, S., Hegedűs, K., Takáts, S. et al. (2017). Rab2 promotes autophagic and endocytic lysosomal degradation. *J. Cell Biol.* **216**, 1937-1947.

Mizushima, N., Levine, B., Cuervo, A. M. and Klionsky, D. J. (2008). Autophagy fights disease through cellular self-digestion. *Nature* **451**, 1069-1075.

Morita, S., Kojima, T. and Kitamura, T. (2000). Plat-E: an efficient and stable system for transient packaging of retroviruses. *Gene Ther.* **7**, 1063-1066.

Mrozowska, P. S. and Fukuda, M. (2016). Regulation of podocalyxin trafficking by Rab small GTPases in 2D and 3D epithelial cell cultures. *J. Cell Biol.* **213**, 355-369.

Nakamura, S. and Yoshimori, T. (2017). New insights into autophagosome–lysosome fusion. *J. Cell Sci.* **130**, 1209-1216.

Ni, H.-M., Bockus, A., Wozniak, A. L., Jones, K., Weinman, S., Yin, X.-M. and Ding, W.-X. (2011). Dissecting the dynamic turnover of GFP-LC3 in the autolysosome. *Autophagy* **7**, 188-204.

Peña-Llopis, S., Vega-Rubin-de-Celis, S., Schwartz, J. C., Wolff, N. C., Tran, T. A., Zou, L., Xie, X.-J., Corey, D. R. and Brugarolas, J. (2011). Regulation of TFEB and V-ATPases by mTORC1. *EMBO J.* **30**, 3242-3258.

Saitoh, T., Nakayama, M., Nakano, H., Yagita, H., Yamamoto, N. and Yamaoka, S. (2003). TWEAK induces NF-κB2 p100 processing and long lasting NF-κB activation. *J. Biol. Chem.* **278**, 36005-36012.

Settembre, C., Di Malta, C., Polito, V. A., Garcia Arencibia, M., Vetrini, F., Erdin, S., Erdin, S. U., Huynh, T., Medina, D., Colella, P. et al. (2011). TFEB links autophagy to lysosomal biogenesis. *Science* **332**, 1429-1433.

Shen, H.-M. and Mizushima, N. (2014). At the end of the autophagic road: an emerging understanding of lysosomal functions in autophagy. *Trends Biochem. Sci.* **39**, 61-71.

Stransky, L. A. and Forgac, M. (2015). Amino acid availability modulates vacuolar H^+-ATPase assembly. *J. Biol. Chem.* **290**, 27360-27369.

Szatmári, Z. and Sass, M. (2014). The autophagic roles of Rab small GTPases and their upstream regulators. *Autophagy* **10**, 1154-1166.

Takahashi, K., Mashima, H., Miura, K., Maeda, D., Goto, A., Goto, T., Sun-Wada, G.-H., Wada, Y. and Ohnishi, H. (2017). Disruption of small GTPase Rab7 exacerbates the severity of acute pancreatitis in experimental mouse models. *Sci. Rep.* **7**, 2817.

Takáts, S., Nagy, P., Varga, Á., Pircs, K., Kárpáti, M., Varga, K., Kovács, A. L., Hegedűs, K. and Juhász, G. (2013). Autophagosomal Syntaxin17-dependent lysosomal degradation maintains neuronal function in *Drosophila*. *J. Cell Biol.* **201**, 531-539.

Takáts, S., Pircs, K., Nagy, P., Varga, Á., Kárpáti, M., Hegedűs, K., Kramer, H., Kovács, A. L., Sass, M. and Juhász, G. (2014). Interaction of the HOPS complex with Syntaxin 17 mediates autophagosome clearance in *Drosophila*. *Mol. Biol. Cell* **25**, 1338-1354.

Takeshige, K., Baba, M., Tsuboi, S., Noda, T. and Ohsumi, Y. (1992). Autophagy in yeast demonstrated with proteinase-deficient mutants and conditions for its induction. *J. Cell Biol.* **119**, 301-311.

Tan, H. W. S., Sim, A. Y. L. and Long, Y. C. (2017). Glutamine metabolism regulates autophagy-dependent mTORC1 reactivation during amino acid starvation. *Nat. Commun.* **8**, 338.

Tsuboyama, K., Koyama-Honda, I., Sakamaki, Y., Koike, M., Morishita, H. and Mizushima, N. (2016). The ATG conjugation systems are important for degradation of the inner autophagosomal membrane. *Science* **354**, 1036-1041.

Vega-Rubin-de-Celis, S., Peña-Llopis, S., Konda, M. and Brugarolas, J. (2017). Multistep regulation of TFEB by MTORC1. *Autophagy* **13**, 464-472.

Yoshimori, T. (2004). Autophagy: a regulated bulk degradation process inside cells. *Biochem. Biophys. Res. Commun.* **313**, 453-458.

Yu, L., McPhee, C. K., Zheng, L., Mardones, G. A., Rong, Y., Peng, J., Mi, N., Zhao, Y., Liu, Z., Wan, F. et al. (2010). Termination of autophagy and reformation of lysosomes regulated by mTOR. *Nature* **465**, 942-946.

Zhou, J., Tan, S.-H., Nicolas, V., Bauvy, C., Yang, N.-D., Zhang, J., Xue, Y., Codogno, P. and Shen, H.-M. (2013). Activation of lysosomal function in the course of autophagy via mTORC1 suppression and autophagosome–lysosome fusion. *Cell Res.* **23**, 508-523.

Zoncu, R., Efeyan, A. and Sabatini, D. M. (2011). mTOR: from growth signal integration to cancer, diabetes and ageing. *Nat. Rev. Mol. Cell Biol.* **12**, 21-35.